



ELSEVIER

Journal of Organometallic Chemistry 659 (2002) 107–116

Journal
of Organometallic
Chemistry

www.elsevier.com/locate/jorgchem

Synthesis, characterization and structural studies of new heterometallic alkynyl complexes of platinum and Group 11 metals with chelating bis(diphenylphosphino)ferrocene ligand

Wai-Yeung Wong*, Guo-Liang Lu, Ka-Ho Choi

Department of Chemistry, Hong Kong Baptist University, Waterloo Road, Kowloon Tong, Hong Kong, PR China

Received 13 May 2002; received in revised form 1 July 2002; accepted 3 July 2002

Abstract

Reaction of the platinum bis(alkynyl) complex $[\text{Pt}(\text{dppf})(\text{C}\equiv\text{CPh})_2]$ (**1**) (dppf = bis(diphenylphosphino)ferrocene) with an equimolar amount of Group 11 metal salts $[\text{Cu}(\text{NCMe})_4]\text{BF}_4$ and AgBF_4 initially gives 1:1 mixed-metal complexes $[\text{Pt}(\text{dppf})(\text{C}\equiv\text{CPh})_2\text{Cu}(\text{NCMe})]\text{BF}_4$ (**2**) and $[\text{Pt}(\text{dppf})(\text{C}\equiv\text{CPh})_2\text{Ag}]\text{BF}_4$ (**3**) in good yields. Upon standing in solution at room temperature, compounds **2** and **3** rearrange and aggregate to the corresponding diplatinum complexes $[\{\text{Pt}(\text{dppf})(\text{C}\equiv\text{CPh})_2\}_2\text{M}]\text{BF}_4$ ($\text{M} = \text{Cu}$ (**4**), Ag (**5**)) which exhibit an intense molecular ion envelope for the respective cation in their electrospray mass spectra. Compounds **4** and **5** can also be formed when the reaction is performed using a 2:1 molar ratio of **1** and the Group 11 salts. The X-ray crystal structures of **1**, **4** and **5** have been determined. Structures of **4** and **5** reveal that the two square-planar platinum coordination planes in the cation are approximately orthogonal an η^2 -fashion to four carbon–carbon triple bonds to afford heterometallic pentanuclear $\text{Fe}_2\text{Pt}_2\text{M}$ complexes ($\text{M} = \text{Cu}, \text{Ag}$) in which each platinum center is stabilized by a dppf ligand. Each of the new complexes displays a reversible oxidation couple corresponding to the ferrocenyl unit of dppf and there is less stabilization of the silver in the mixed-metal complex than in the copper congeners. © 2002 Elsevier Science B.V. All rights reserved.

Keywords: Copper; Silver; Platinum; Ferrocene; Crystal structures

1. Introduction

The molecular design and synthesis of polynuclear acetylide systems continue to attract considerable current interest because of the unusual structural features and the novel reactivity patterns exhibited by these molecules [1]. In particular, the reaction chemistry of bis(alkynyl) metal complexes $\text{R}^1\text{—C}\equiv\text{C—}[\text{M}]\text{—C}\equiv\text{C—R}^2$ towards different transition metal centers (electron-rich or -deficient) species has been extensively studied [1a,2]. A vast range of coordination modes of the alkynyl ligands are found in these systems which depend on the nature of the alkynyl substituents, the auxiliary ligands and the metal centers involved [1a,3]. Among these, tweezer-type transition metal bis(alkynyl) precursor complexes in a *cis* configuration are widely exploited

as organometallic chelating ligands in the formation of novel homo- or hetero-bimetallic molecules, where the second metal is bonded in an η^2 -fashion to the alkynyl $\text{C}\equiv\text{C}$ triple bonds [1a,3]. In this context, the most widely investigated complexes are mainly based either upon the bis(cyclopentadienyl)titanium system [1a,2a,2b,2d], or upon *cis*-platinum systems with imines, tertiary phosphines or C_6F_5 entity as the auxiliary groups [1a,2e]. These bimetallic complexes have been shown to display interesting chemical and physical properties. Although there are numerous reports on the use of *cis*- $[\text{PtL}_2(\text{C}\equiv\text{CR})_2]$ precursors ($\text{L} = \text{PPh}_3$, $\text{L}_2 = \text{dppe}$, *bipy*, substituted *bipy*; $\text{R} = \text{SiMe}_3$, *Ph*, *t*-*Bu*, etc.) to form tweezer-like complexes [1a,2], organometallic chelating ligands such as bis(diphenylphosphino)ferrocene (dppf) are, to our knowledge, rarely employed in such study. Dppf ligand is expected to impart strikingly different properties to these systems from the purely organic moieties or metal-free phosphine groups, particularly with respect to their spectroscopic and redox behavior [4].

* Corresponding author. Tel.: +852-3411-7074; fax: +852-3411-7348

E-mail address: rwywong@hkbu.edu.hk (W.-Y. Wong).

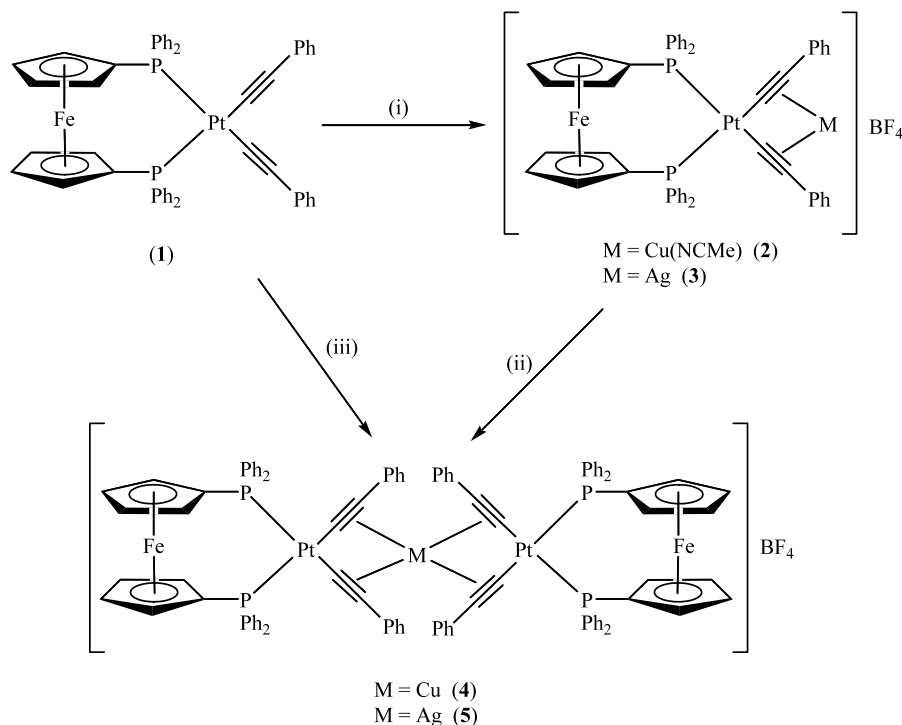
Recently, we have reported the preparation of two novel heterotetranuclear carbonyl clusters $[\text{Os}_3\text{Pt}(\text{CO})_9(\mu_4\text{-}\eta^2\text{-C}\equiv\text{CPh})(\eta^1\text{-C}\equiv\text{CPh})(\text{L-L})]$ ($\text{L-L} = 4,4'$ -dimethyl-2,2'-bipyridine, 4,4'-bis(*tert*-butyl)-2,2'-bipyridine) from the reactions of $[\text{Os}_3(\text{CO})_{10}(\text{NCMe})_2]$ with the molecular tweezers $[\text{Pt}(\text{L-L})(\text{C}\equiv\text{CPh})_2]$ [5]. In line with our efforts to develop other assembled multi-metallic systems involving platinum bis(alkynyl) complexes [6], we utilize the dppf-stabilized complex $[\text{Pt}(\text{dppf})(\text{C}\equiv\text{CPh})_2]$ (**1**) as a starting precursor for the encapsulation of low-valent Group 11 transition metals, which may provide synthetic access to some multi-metallic compounds. The chelating dppf ligand was chosen due to its large steric strain in square-planar Pt complexes, which ensures a *cis* configuration. We describe here the reactions of **1** with some Group 11 metal salts $[\text{Cu}(\text{NCMe})_4]\text{BF}_4$ and AgBF_4 and the structural characterizations of new mixed-metal pentanuclear $\text{Fe}_2\text{Pt}_2\text{M}$ complexes $[\{\text{Pt}(\text{dppf})(\text{C}\equiv\text{CPh})_2\}_2\text{-M}]\text{BF}_4$ ($\text{M} = \text{Cu}, \text{Ag}$) are described.

2. Results and discussion

2.1. Synthesis and spectroscopic characterization

The results of the reactions are summarized in Scheme 1. In accordance with the synthetic strategy for making the complexes $[\text{Pt}(\text{diimine})(\text{C}\equiv\text{C}\text{Ar})_2]$, complex $[\text{Pt}(\text{dppf})(\text{C}\equiv\text{CPh})_2]$ (**1**) is readily prepared by a CuI-

catalyzed chloride-to-alkyne metathesis reaction between $[\text{Pt}(\text{dppf})\text{Cl}_2]$ and $\text{PhC}\equiv\text{CH}$ in the CuI–amine system [7]. An improved synthesis leading to $[\text{Pt}(\text{dppf})\text{Cl}_2]$ [8] was employed which involves treatment of $[\text{PtCl}_2(\text{SEt}_2)_2]$ [9] with dppf in CH_2Cl_2 at room temperature. The yield and purity of **1** is similar to that reported by Dias and coworkers [10]. The 1:1 trimetallic complexes $[\text{Pt}(\text{dppf})(\text{C}\equiv\text{CPh})_2\text{Cu}(\text{NCMe})]\text{BF}_4$ (**2**) and $[\text{Pt}(\text{dppf})(\text{C}\equiv\text{CPh})_2\text{Ag}]\text{BF}_4$ (**3**) were synthesized in almost quantitative yields by the room temperature reaction of the platinum bis(alkynyl) precursor **1** in chloroform with a stoichiometric amount of $[\text{Cu}(\text{NCMe})_4]\text{BF}_4$ and AgBF_4 , respectively, in acetonitrile. Pure **2** and **3** are stable as solids, but are prone to undergo rearrangement reactions after prolonged periods in solutions. Upon standing in solutions, compounds **2** and **3** rearrange to the corresponding 2:1 mixed-metal pentanuclear aggregates $[\{\text{Pt}(\text{dppf})(\text{C}\equiv\text{CPh})_2\}_2\text{M}]\text{BF}_4$ ($\text{M} = \text{Cu}$ (**4**), Ag (**5**)). Similar treatment of **1** with 0.5 equivalent of Group 11 metal salts in the same solvent combination led to the isolation of **4** and **5** in high purity and yields. New complexes **2–5** are soluble in common organic solvents and have been characterized by satisfactory microanalysis, IR and NMR spectroscopies (Section 4). The identities of **2** and **3** were also supported by fast atom bombardment mass spectrometry (FAB-MS) and **4** and **5** by electrospray ionization mass spectrometry (ESI-MS). The molecular structures of **1**, **4** and **5** have been established by X-ray crystallography (vide infra).



Scheme 1. (i) 1 equivalent $[\text{Cu}(\text{NCMe})_4]\text{BF}_4$ or AgBF_4 , $\text{CHCl}_3\text{-MeCN}$. (ii) $\text{CH}_2\text{Cl}_2\text{-hexane}$, room temperature. (iii) 0.5 equivalent $[\text{Cu}(\text{NCMe})_4]\text{BF}_4$ or AgBF_4 , $\text{CHCl}_3\text{-MeCN}$.

In the solid state IR spectra, complex **1** shows two $\text{C}\equiv\text{C}$ stretching vibrations at ca. 2112 and 2120 cm^{-1} whereas compounds **3** and **5** display a very weak $\nu_{\text{C}=\text{C}}$ absorption at the lower wavenumber region than **1** because of the η^2 -coordination of the alkyne at the silver atom [1a]. However, we cannot observe the corresponding peaks for the copper analogues. The $^1\text{H-NMR}$ spectra of diamagnetic compounds **2–5** consist of well-resolved signals for each of the organic and ferrocenyl groupings present. Their spectroscopic data show close resemblance to those found in the parent complex **1**, although small differences in chemical shifts are observed. The sharp singlet peak at δ 1.97 for **2** is due to the coordinated acetonitrile molecule, in agreement with the monomeric structure of **2** in solution initially. The retention of the phosphines is evident from the $^{31}\text{P-NMR}$ spectrum in each case, which shows a strong singlet flanked by two platinum satellites, and the values

of $^1J_{\text{Pt-P}}$ (2506–2648 Hz) are consistent with a *cis* configuration for the phosphines and for the acetylides about platinum [7b,10,11]. The FAB-MS data for **3** and **4** showed peaks corresponding to the $[\text{M-MeCN-BF}_4]^+$ and $[\text{M-BF}_4]^+$ fragments, respectively. The formulae of the larger complexes **4** and **5** were studied by the electrospray mass spectrometric technique with methanol as the mobile phase. The ESI-MS spectra of **4** and **5** exhibited an intense parent peak for the cation at m/z 1966 and 2011, respectively, which match very well with the calculated isotopic distribution patterns (Figs. 1 and 2). The soft ionization mode in ESI-MS reduces the degree of fragmentation as compared with other common ionization methods (e.g. EI or FAB), which can maximize the population of target species to enter the ion trap.

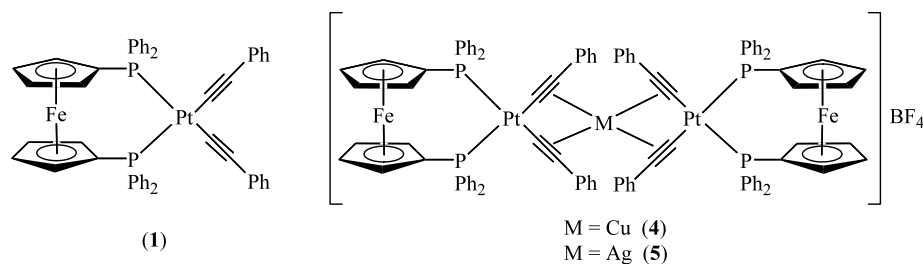


Chart 1

of $^1J_{\text{Pt-P}}$ (2506–2648 Hz) are consistent with a *cis* configuration for the phosphines and for the acetylides about platinum [7b,10,11]. The FAB-MS data for **3** and **4** showed peaks corresponding to the $[\text{M-MeCN-BF}_4]^+$ and $[\text{M-BF}_4]^+$ fragments, respectively. The formulae of the larger complexes **4** and **5** were studied by the electrospray mass spectrometric technique with methanol as the mobile phase. The ESI-MS spectra of **4** and **5** exhibited an intense parent peak for the cation at m/z 1966 and 2011, respectively, which match very well with the calculated isotopic distribution patterns (Figs. 1 and 2). The soft ionization mode in ESI-MS reduces the degree of fragmentation as compared with other common ionization methods (e.g. EI or FAB), which can maximize the population of target species to enter the ion trap.

2.2. Crystal structure analyses

Single-crystal X-ray analyses were carried out for **1**, **4** and **5** to ascertain their solid-state structures (Chart 1). A perspective view of the molecular structure of **1** is depicted in Fig. 3, which includes the atom-numbering

X-Ray crystallographic analysis on **4** reveals that the structure contains the cationic pentanuclear unit $[\{\text{Pt}(\text{dppf})(\text{C}\equiv\text{CPh})_2\}_2\text{Cu}]^+$ and a drawing of the cation is illustrated in Fig. 4 along with selected bond parameters shown in Table 2. The cation is formed by two nearly orthogonal $\text{Pt}(\text{dppf})(\text{C}\equiv\text{CPh})_2$ units (the dihedral angle between the best-squares coordination planes PtP_2C_2 being 85.9°) bridged by a monomeric copper ion. Each of the two $\text{Pt}(\text{dppf})(\text{C}\equiv\text{CPh})_2$ units possesses an essentially square-planar platinum center and behaves as a bidentate chelating ligand for the copper entity. The geometric details of the two $\text{Pt}(\text{dppf})$ moieties in **4** are similar to those reported for **1**. The Pt–P distances vary from 2.300(2) to 2.323(2) Å and the Pt–C distances are in the expected range quoted in the literature for σ -alkynylplatinum compounds [7b,12,13]. The central metal atom adopts an approximately tetrahedral arrangement and is η^2 -coordinated to four alkyne groups with slightly shorter distances to the β -carbon than to the α -carbon atoms of the ethynyl groups (mean α -distances 2.228(7), β -distances 2.350(7) Å) [1a]. These Cu–C(alkyne) distances are comparable to those found in $[\{\text{Pt}(\text{dppe})(\text{C}\equiv\text{CPh})_2\}_2\text{Cu}]\text{BF}_4$

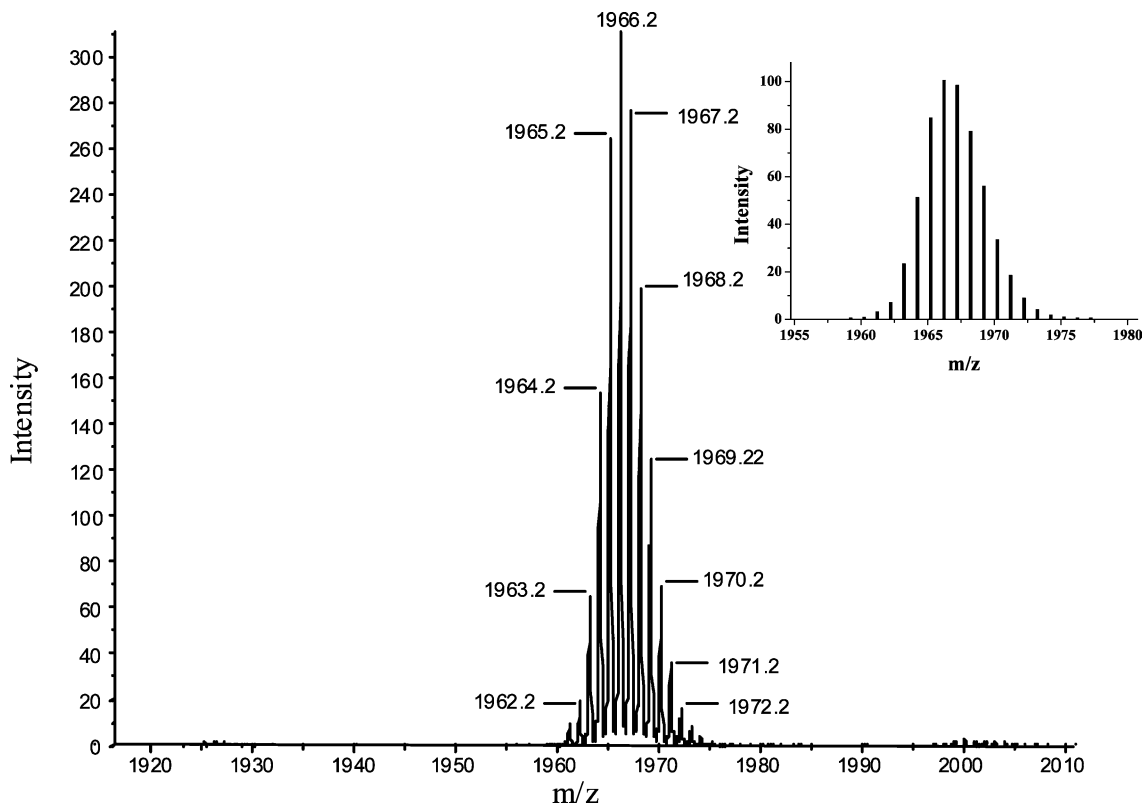


Fig. 1. The ESI mass spectrum of **4** recorded in MeOH. The inset shows the simulated isotopic mass pattern.

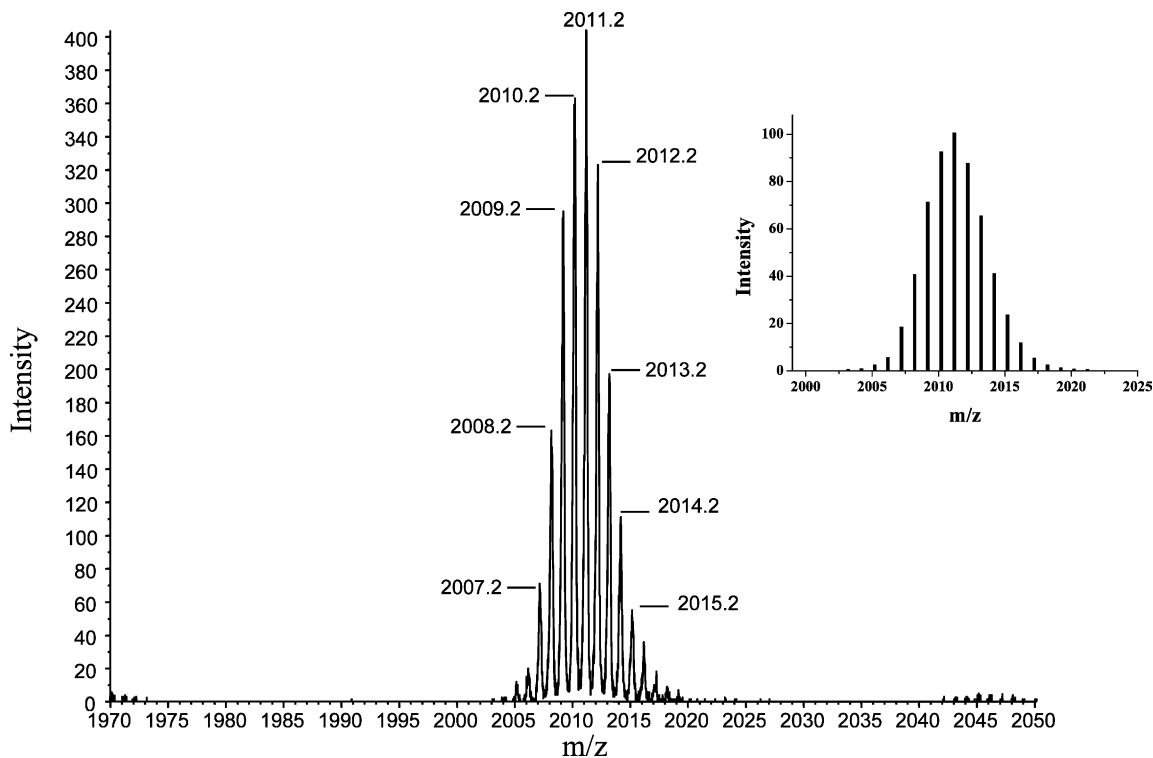


Fig. 2. The ESI mass spectrum of **5** recorded in MeOH. The inset shows the simulated isotopic mass pattern.

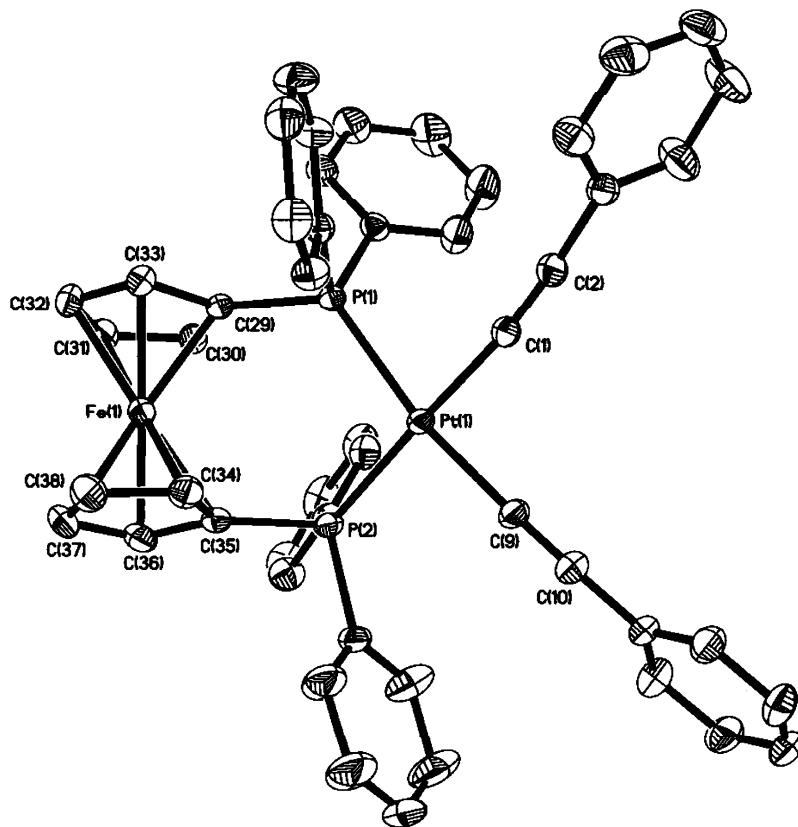


Fig. 3. Molecular structure of **1**, showing the atomic labelling scheme. Labels on the phenyl rings and all hydrogen atoms have been omitted for clarity.

Table 1
Selected bond lengths (Å) and angles (°) for compound **1**·C₄H₈O

Bond lengths			
Pt(1)–P(1)	2.3109(4)	Pt(1)–P(2)	2.3008(4)
Pt(1)–C(1)	2.0045(16)	Pt(1)–C(9)	1.9943(15)
C(1)–C(2)	1.195(2)	C(9)–C(10)	1.199(2)
Bond angles			
P(1)–Pt(1)–P(2)	100.025(14)	C(1)–Pt(1)–C(9)	88.48(7)
Pt(1)–C(1)–C(2)	173.20(14)	Pt(1)–C(9)–C(10)	176.66(16)
C(1)–C(2)–C(3)	176.331(18)	C(9)–C(10)–C(11)	177.4(2)

(2.19(3)–2.49(3) Å) [14]. The Cu atom lies 0.2145 Å out of the Pt(1)–P(1)–P(2) plane and 0.3179 Å out of the Pt(2)–P(3)–P(4) plane. The geometries of the Pt(C≡CPh)Cu bridges are normal and similar to those in derivatives of the general type [Pt(L–L)(C≡CR)₂M]X (L–L = diimines, mono- or bidentate phosphines; R = SiMe₃, Ph, ^tBu; M = Cu, Cu(NCMe); X = Cl, SCN, BF₄, ClO₄, etc.) [1a,2e,14]. As a result of the η²-coordination of each alkynyl ligand in **4** to the Cu center, we note a bending of the C≡C–Ph units from 176.3(2)–177.4(2)° in **1** to 167.5(8)–173.1(8)° in **4**. The bite angle C_α–Pt–C_α also decreases slightly from 88.48(7)° in **1** to the mean value of ca. 87.1(3)° in **4** [1a]. The absence of metal–metal interactions in this

mixed copper–platinum complex was indicated from the Pt(1)···Cu (3.171 Å) and Pt(2)···Cu (3.217 Å) distances, reminiscent of other similar compounds [1a,2e,14]. As far as the phosphinoferoctenyl groups are concerned, the cyclopentadienyl rings of each ferrocenyl unit are almost planar (mean deviation of ca. 0.0035–0.0061 Å) and the tilt angle is 3.1° in each case. The C₅H₄ fragments of the ferrocenyl group deviate from the staggered configuration by 1.4 and 2.7° for the Fe(1) and Fe(2) units, respectively. The mean Fe–C(C₅H₄) bond length is 2.028 Å and the C₅H₄ rings produce an average distance of 1.6257 and 1.6379 Å from their centroids to Fe(1) and Fe(2), respectively.

A partial determination of the molecular structure of **5** was made; the cation of which is depicted in Fig. 5. Preliminary X-ray study is consistent with the proposed structure but the poor quality of the data as well as the severe disorder problem encountered for the anion precludes discussion of the structural details. Generally speaking, the structure of **5** is very similar to that of **4**, except that Cu(I) is being replaced by Ag(I) and the structural parameters are rather close to those observed for [Pt(PPh₃)₂(C≡CPh)₄]Ag[ClO₄] [15]. Again, the intramolecular contacts between Pt and Ag atoms in **5** (> 3.3 Å) are well outside the range for any direct metal–metal interactions.

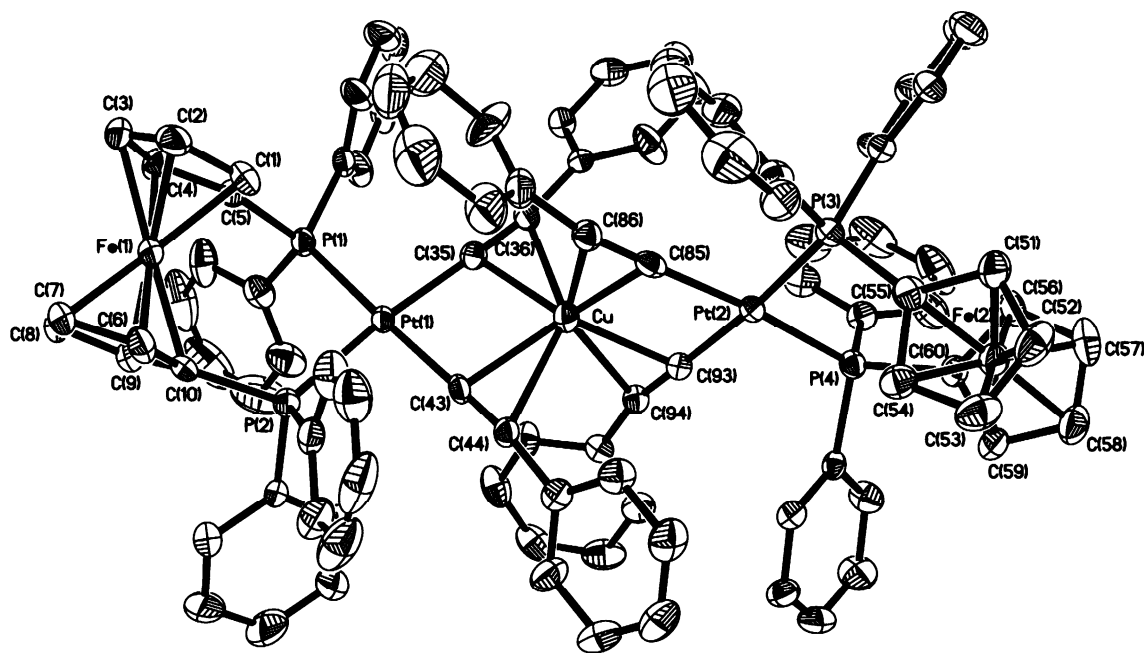


Fig. 4. Molecular structure of the cation of **4**, showing the atomic labelling scheme. Labels on the phenyl rings and all hydrogen atoms have been omitted for clarity.

Table 2
Selected bond lengths (Å) and angles (°) for compound **4**

Bond lengths			
Pt(1)–P(1)	2.300(2)	Pt(1)–P(2)	2.323(2)
Pt(2)–P(3)	2.3018(19)	Pt(2)–P(4)	2.3223(19)
Pt(1)–C(35)	2.025(8)	Pt(1)–C(43)	2.012(8)
Pt(2)–C(85)	2.021(9)	Pt(2)–C(93)	2.014(7)
Cu–C(35)	2.227(7)	Cu–C(36)	2.336(7)
Cu–C(43)	2.242(6)	Cu–C(44)	2.415(7)
Cu–C(85)	2.247(7)	Cu–C(86)	2.350(8)
Cu–C(93)	2.196(7)	Cu–C(94)	2.300(7)
C(35)–C(36)	1.194(8)	C(43)–C(44)	1.186(9)
C(85)–C(86)	1.206(9)	C(93)–C(94)	1.209(8)
Bond angles			
P(1)–Pt(1)–P(2)	97.63(7)	P(3)–Pt(2)–P(4)	98.23(7)
C(35)–Pt(1)–C(43)	88.4(3)	C(85)–Pt(2)–C(93)	85.8(3)
Pt(1)–C(35)–C(36)	172.8(7)	Pt(1)–C(43)–C(44)	178.3(7)
Pt(2)–C(85)–C(86)	175.7(7)	Pt(2)–C(93)–C(94)	178.7(6)
C(35)–C(36)–C(37)	169.3(8)	C(43)–C(44)–C(45)	173.1(8)
C(85)–C(86)–C(87)	169.1(8)	C(93)–C(94)–C(95)	167.5(8)
Pt(1)–C(35)–Cu	96.7(3)	Pt(1)–C(43)–Cu	96.6(3)
Pt(2)–C(85)–Cu	97.7(3)	Pt(2)–C(93)–Cu	99.5(3)

2.3. Electrochemistry

The electrochemical properties of our new complexes were investigated by cyclic voltammetry in CH_2Cl_2 at room temperature (r.t.) and the redox data are gathered in Table 3. In each case, the cyclic voltammogram is characterized by a single quasi-reversible oxidation wave due to the ferrocenyl electrophore that is present in the complex. The oxidation wave for **4** and **5** corresponds to

the single-step two-electron oxidation involving the concomitant oxidation of the two terminal ferrocenyl groups [6a,16]. The possibility that this oxidation event is due to the $\text{M}^{\text{I}} \rightarrow \text{M}^{\text{II}}$ couple can be ruled out since the oxidized $\text{M}(\text{II})$ species ($\text{M} = \text{Cu}, \text{Ag}$) does not favour coordination by the acetylide bridges, making the process irreversible [2e]. An anodic shift of the ferrocene-ferrocenium couple in **1** with reference to $[\text{Pt}(\text{dppf})\text{Cl}_2]$ is consistent with the unsaturation of the ethynyl group which makes the removal of electrons more difficult. Upon complexation with Group 11 metal ions, the ferrocenyl redox potential shows a negative shift of ca. 0.20–0.26 V which is in line with the stronger electron donation from the ferrocenyl moiety to stabilize the positive charge on the $\text{M}(\text{I})$ ion. With each Group 11 metal, there is only a small difference in the potential values between the 1:1 and 2:1 mixed-metal complexes. The higher oxidation potentials for the silver complexes than for the copper counterparts suggest that there should be less stabilization of the silver in the complexes than in the copper complexes [2e]. Another redox event was also observed at +0.52 V for **1** which is attributable to the $\text{Pt}^{\text{II}} \rightarrow \text{Pt}^{\text{III}}$ irreversible oxidation. However, no such anodic wave was associated with the mixed-metal compounds **2–5**.

3. Concluding remarks

This report demonstrates the successful use of dppf -stabilized platinum bis(alkynyl) precursor **1** as bidentate complexing agents for the stabilization of low oxidation

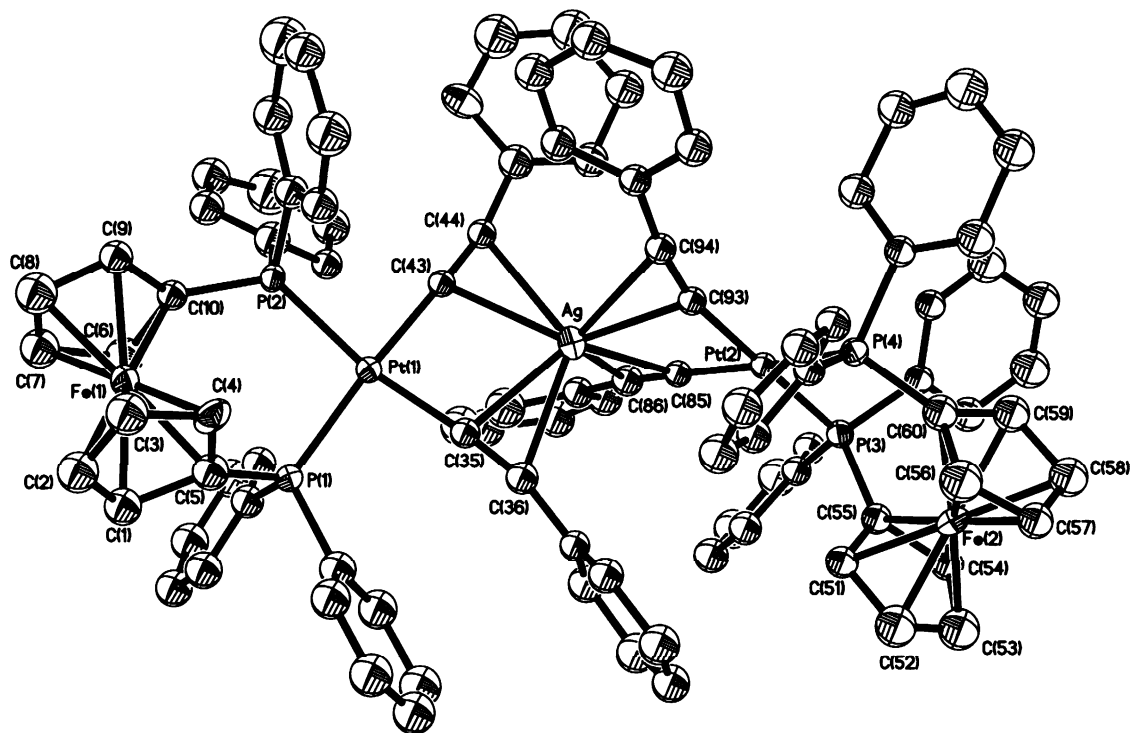


Fig. 5. Molecular structure of the cation of **5**, showing the atomic labelling scheme. Labels on the phenyl rings and all hydrogen atoms have been omitted for clarity.

Table 3
Redox data for the dppf-stabilized platinum bis(alkynyl) complexes in CH_2Cl_2

Complex	$E_{1/2}$ (V) ^a
[Pt(dppf)Cl ₂]	0.60 (99)
1	0.52 ^b , 0.83 (138)
2	0.60 (99)
3	0.63 (99)
4	0.57 (99)
5	0.59 (119)

^a Scan rate = 100 mV s^{-1} , half-wave potential values $E_{1/2} = (E_{\text{pa}} + E_{\text{pc}})/2$ for reversible oxidation, $\Delta E_{\text{p}} = E_{\text{pa}} - E_{\text{pc}}$ (in mV) for reversible waves are given in parentheses, where E_{pa} and E_{pc} are the anodic and cathodic peak potentials, respectively.

^b Irreversible wave.

state Group 11 metal moieties. Starting with **1**, some new 1:1 and 2:1 mixed-metal complexes of platinum and Group 11 metals bridged by alkynyl ligands in an η^2 -manner were prepared and spectroscopically characterized. Even in the presence of bulky dppf ligands, aggregation into the larger 2:1 species is possible and positive-mode electrospray mass spectrometric and X-ray crystal structure analyses unequivocally establish the identity of the complexes $[\{\text{Pt}(\text{dppf})(\text{C}\equiv\text{CPh})_2\}_2\text{M}]\text{BF}_4$ (M = Cu (**4**), Ag (**5**)) to be a 2:1 Pt/M stoichiometry.

4. Experimental

4.1. General procedures

All reactions were carried out under N_2 with the use of standard inert atmosphere and Schlenk techniques, but no special precautions were taken to exclude oxygen during work-up. Solvents were predried and distilled from appropriate drying agents [17]. All chemicals, unless otherwise stated, were obtained from commercial sources and used as received. The compound $[\text{Cu}(\text{NCMe})_4]\text{BF}_4$ was prepared according to the published literature method [18]. Infrared spectra were recorded as KBr pellets on a Perkin–Elmer Paragon 1000 PC or Nicolet Magna 550 Series II FTIR spectrometer. NMR spectra were measured in CDCl_3 on a JEOL EX270 or a Varian INOVA 400 MHz FT NMR spectrometer. ^1H -NMR chemical shifts were quoted relative to SiMe_4 ($\delta = 0$) and ^{31}P chemical shifts relative to an 85% H_3PO_4 external standard. Positive FAB mass spectra were recorded on a Finnigan MAT SSQ710 mass spectrometer. The ESI mass spectrometry experiments were performed on a PE SCIEX API QSTAR PULSAR i mass spectrometer. Mass spectra of compounds **4** and **5** were acquired in the positive-ion detection mode using methanol as the mobile phase and the sample was injected at the rate of $10 \mu\text{l min}^{-1}$. The ion spray voltage of the ESI source was set at 5.5 kV. Electronic absorption spectra were obtained with a Hewlett Pack-

ard 8453 UV–vis spectrometer. Cyclic voltammetry experiments were done with a Princeton Applied Research (PAR) model 273A potentiostat. A conventional three-electrode configuration consisting of a glassy-carbon working electrode, a Pt-wire counter electrode and a Ag/AgNO₃ reference electrode (0.1 M in MeCN) was used. The solvent in all measurements was deoxygenated CH₂Cl₂ and the supporting electrolyte was 0.1 M [Bu₄N]PF₆. Ferrocene was added as a calibrant after each set of measurements and all potentials reported were quoted with reference to the ferrocene–ferrocenium couple. The number of electrons transferred for **4** and **5** was estimated by comparing the peak height of the respective ferrocene oxidation wave with an equal concentration of the ferrocene standard added in the same system, in which one-electron oxidation was assumed.

4.2. Complex preparations

4.2.1. Synthesis of [Pt(dppf)Cl₂]

This compound was prepared by a modification of the literature method [8]. To a suspension of PtCl₂ (266.0 mg, 1.00 mmol) in CH₂Cl₂ (10 ml), SET₂ (0.32 ml, 3.00 mmol) was added to give a clear yellow solution of [PtCl₂(SET₂)₂]. After the solution was stirred for 0.5 h, dppf (555.0 mg, 1.00 mmol) was added and the resulting brown solution was stirred for an additional 0.5 h. The solvent was then removed under reduced pressure and the residue washed with a mixture of CH₂Cl₂ and C₆H₁₄ (1:1, v/v) to afford a yellow powder of [Pt(dppf)Cl₂] (96%, 788.0 mg). ¹H-NMR (CDCl₃): δ 4.18 (s, 4H, C₅H₄), 4.36 (s, 4H, C₅H₄), 7.34–7.49 (m, 12H, Ph), 7.82–7.89 (m, 8H, Ph). ³¹P{¹H}-NMR (CDCl₃): δ 14.54 (¹J_{Pt–P} = 3755 Hz). FAB-MS (*m/z*): 820 [M]⁺. Anal. Found: C, 49.60; H, 3.11. C₃₄H₂₈Cl₂FeP₂Pt requires C, 49.78; H, 3.44%.

4.2.2. Synthesis of [Pt(dppf)(C≡CPh)₂] (**1**)

Phenylacetylene (153.0 mg, 1.50 mmol) was added to a suspension of [Pt(dppf)Cl₂] (410.0 mg, 0.50 mmol) and CuI (20 mg) in ¹Pr₂NH (25 ml) and CH₂Cl₂ (25 ml). The mixture was stirred overnight (16 h) at r.t., during which time it turned to a milky suspension. After filtration, the solid was washed with MeCN and CH₂Cl₂, dissolved in a little hot CHCl₃ and subjected to a short silica column using CH₂Cl₂ as eluent. From the first yellow band, a light yellow solid of **1** was obtained in 63% yield (300.0 mg). IR (KBr, cm⁻¹): 2112m, 2120m (ν_{C≡C}). ¹H-NMR (CDCl₃): δ 4.19 (s, 4H, C₅H₄), 4.31 (s, 4H, C₅H₄), 6.77–6.81 (m, 4H, C≡CPh), 6.96–7.00 (m, 6H, C≡CPh), 7.27–7.40 (m, 12H, Ph), 7.81–7.88 (m, 8H, Ph). ³¹P{¹H}-NMR (CDCl₃): δ 15.95 (¹J_{Pt–P} = 2365 Hz). FAB-MS (*m/z*): 952 [M]⁺. Anal. Found: C, 63.02; H, 3.91. C₅₀H₃₈FeP₂Pt requires C, 63.10; H, 4.02%.

4.2.3. Synthesis of [Pt(dppf)(C≡CPh)₂Cu(NCMe)]BF₄ (**2**) and [Pt(dppf)(C≡CPh)₂]₂Cu]BF₄ (**4**)

To a solution of [Pt(dppf)(C≡CPh)₂] (9.5 mg, 0.01 mmol) in CHCl₃ (5 ml) was added a solution of [Cu(NCMe)₄]BF₄ (3.5 mg, 0.01 mmol) in MeCN (1 ml). After the mixture was stirred for 1 h at r.t., all the volatile components were removed under reduced pressure. The residue was taken up in CHCl₃ and filtered. Removal of the solvents gave **2** as a bright yellow solid in almost quantitative yield (98%, 11.2 mg). ¹H-NMR (CDCl₃): δ 1.97 (s, 3H, MeCN), 4.23 (s, 4H, C₅H₄), 4.45 (s, 4H, C₅H₄), 6.66–6.69 (m, 4H, C≡CPh), 7.07–7.12 (m, 6H, C≡CPh), 7.32–7.45 (m, 12H, Ph), 7.69–7.76 (m, 8H, Ph). ³¹P{¹H}-NMR (CDCl₃): δ 14.12 (¹J_{Pt–P} = 2646 Hz). FAB-MS (*m/z*): 1015 [M–MeCN–BF₄]⁺. Anal. Found: C, 54.50; H, 3.42; N, 1.04. C₅₂H₄₁NBCuF₄–FeP₂Pt requires C, 54.64; H, 3.62; N, 1.23%. A solution of compound **2** in a mixture of CH₂Cl₂ and C₆H₁₄ was slowly evaporated at r.t., leading to a deposit of lemon-yellow crystals of **4** after 1 day (yield 80%). ¹H-NMR (CDCl₃): δ 3.97 (s, 8H, C₅H₄), 4.35 (s, 8H, C₅H₄), 6.91–6.93 (m, 8H, C≡CPh), 7.11–7.17 (m, 12H, C≡CPh), 7.22–7.36 (m, 24H, Ph), 7.43–7.48 (m, 16H, Ph). ³¹P{¹H}-NMR (CDCl₃): δ 14.27 (¹J_{Pt–P} = 2559 Hz). ESI-MS (*m/z*): 1966 [M–BF₄]⁺. Anal. Found: C, 58.26; H, 3.58. C₁₀₀H₇₆BCuF₄Fe₂P₄Pt₂ requires C, 58.48; H, 3.73%.

4.2.4. Synthesis of [Pt(dppf)(C≡CPh)₂Ag]BF₄ (**3**) and [Pt(dppf)(C≡CPh)₂]₂Ag]BF₄ (**5**)

Complex **3** was prepared using the same conditions described above for **2**, but AgBF₄ (2.2 mg, 0.01 mmol) was used instead to produce a bright yellow solid of **3** in 96% yield (11.0 mg). IR (KBr, cm⁻¹): 2075vw (ν_{C≡C}). ¹H-NMR (CDCl₃): δ 4.22 (s, 4H, C₅H₄), 4.43 (s, 4H, C₅H₄), 6.89–6.92 (m, 4H, C≡CPh), 7.14–7.23 (m, 6H, C≡CPh), 7.34–7.42 (m, 12H, Ph), 7.68–7.75 (m, 8H, Ph). ³¹P{¹H}-NMR (CDCl₃): δ 12.93 (¹J_{Pt–P} = 2648 Hz). FAB-MS (*m/z*): 1059 [M–BF₄]⁺. Anal. Found: C, 52.07; H, 3.04. C₅₀H₃₈AgBF₄FeP₂Pt requires C, 52.39; H, 3.34%. Upon standing a solution of **3** in a CH₂Cl₂–C₆H₁₄ mixture, tiny yellow crystals were formed after 1 day which was characterized as compound **5** (yield: 77%). IR (KBr, cm⁻¹): 2078w (ν_{C≡C}). ¹H-NMR (CDCl₃): δ 3.97 (s, 8H, C₅H₄), 4.34 (s, 8H, C₅H₄), 6.73–6.75 (m, 8H, C≡CPh), 6.95–6.99 (m, 12H, C≡CPh), 7.05–7.34 (m, 24H, Ph), 7.56–7.60 (m, 16H, Ph). ³¹P{¹H}-NMR (CDCl₃): δ 14.21 (¹J_{Pt–P} = 2506 Hz). ESI-MS (*m/z*): 2011 [M–BF₄]⁺. Anal. Found: C, 56.98; H, 3.44. C₁₀₀H₇₆AgBF₄Fe₂P₄Pt₂ requires C, 57.25; H, 3.65%.

Table 4
Summary of crystal structure data for complexes **1**·C₄H₈O, **4** and **5**

	1 ·C ₄ H ₈ O	4	5
Empirical formula	C ₅₄ H ₄₆ FeOP ₂ Pt	C ₁₀₀ H ₇₆ BCuF ₄ Fe ₂ P ₄ Pt ₂	C ₁₀₀ H ₇₆ AgBF ₄ Fe ₂ P ₄ Pt ₂
Molecular weight	1023.79	2053.72	2098.12
Crystal system	Monoclinic	Monoclinic	Triclinic
Space group	<i>P</i> 2 ₁ / <i>n</i>	<i>P</i> 2 ₁ / <i>n</i>	<i>P</i> $\bar{1}$
<i>a</i> (Å)	12.7678(9)	23.0719(12)	14.8883(15)
<i>b</i> (Å)	21.6216(15)	13.9947(8)	17.6379(17)
<i>c</i> (Å)	16.3142(11)	26.9575(14)	18.6819(19)
α (°)	90	90	84.228(2)
β (°)	98.1040(10)	91.3340(10)	84.668(2)
γ (°)	90	90	75.658(2)
<i>U</i> (Å ³)	4458.7(5)	8701.8(8)	4717.1(8)
<i>Z</i>	4	4	2
μ (Mo–K α) (cm ⁻¹)	3.570	3.899	
<i>F</i> (000)	2048	4056	2064
Crystal size (mm)	0.30 × 0.26 × 0.22	0.33 × 0.14 × 0.09	0.27 × 0.13 × 0.08
θ Range (°)	1.87–27.51	1.77–27.52	1.42–27.55
Reflections collected	25 893	50 486	28 388
Unique reflections	10 008	19 519	20 538
Observed reflections [<i>I</i> > 2 σ (<i>I</i>)]	10 008	19 519	20 538
Parameters	533	1028	
<i>R</i> _{int}	0.0221	0.0972	0.1211
<i>R</i> ₁ , <i>wR</i> ₂ [<i>I</i> > 2 σ (<i>I</i>)]	0.0200, 0.0490	0.0448, 0.0760	0.1057, 0.2633
<i>R</i> ₁ , <i>wR</i> ₂ (all data)	0.0267, 0.0514	0.1485, 0.0974	
Goodness-of-fit	0.927	0.851	0.949
Residual extrema in final difference map (e Å ⁻³)	0.534 to –0.401	1.049 to –0.691	

5. Crystallography

Single crystals of **1**·C₄H₈O suitable for X-ray crystallographic analyses were grown by slow evaporation of its solution in THF–hexane and those of **4** and **5** in hexane–CH₂Cl₂ at room temperature. The crystals for **1** and **4** were glued on a glass fiber with epoxy resin while that for **5** was mounted in a glass capillary. Crystal data and other experimental details are summarized in Table 4. (For **5**, only the cell parameters and some details of the refinement are shown.) The diffraction experiments were carried out at room temperature on a Bruker Axs SMART 1000 CCD area-detector diffractometer using graphite-monochromated Mo–K α radiation ($\lambda = 0.71073$ Å). The collected frames were processed with the software SAINT [19a] and an absorption correction was applied (SADABS [19b]) to the collected reflections.

The space groups for all crystals were determined from a combination of Laue symmetry check and their systematic absences, which were then confirmed by successful refinement of the structures. The structures were solved by direct methods (SHELXTL [20]) in conjunction with standard Fourier difference techniques and subsequently refined by full-matrix least-squares analyses. All non-hydrogen atoms were refined with anisotropic displacement parameters for **1** and **4**. The hydrogen atoms were placed in their ideal positions but not refined.

6. Supplementary material

Crystallographic data (comprising hydrogen atom coordinates, thermal parameters and full tables of bond lengths and angles) for the structural analysis has been deposited with the Cambridge Crystallographic Centre, CCDC nos. 185415 and 185416 for compounds **1** and **4** respectively. Copies of this information may be obtained free of charge from The Director, CCDC, 12 Union Road, Cambridge CB2 1EZ, UK (Fax: +44-1223-336033; e-mail: deposit@ccdc.cam.ac.uk or www: <http://www.ccdc.cam.ac.uk>).

Acknowledgements

Financial support from the Hong Kong Baptist University is gratefully acknowledged. We also thank the Hong Kong Research Grants Council for the purchase of LC-MS instrument for the electrospray mass spectral analyses.

References

- [1] (a) H. Lang, D.S.A. George, G. Rheinwald, *Coord. Chem. Rev.* 206–207 (2000) 101 (and references cited therein);
(b) P.R. Raithby, M.J. Rosales, *Adv. Inorg. Chem. Radiochem.* 29 (1985) 169;
(c) M.I. Bruce, *Chem. Rev.* 91 (1991) 197;

- (d) H. Lang, K. Köhler, S. Blau, *Coord. Chem. Rev.* 143 (1995) 113;
- (e) I. Manners, *Angew. Chem. Int. Ed. Engl.* 35 (1996) 1602;
- (f) S. Lotz, P.H. van Rooyen, R. Meyer, *Adv. Organomet. Chem.* 37 (1995) 219;
- (g) G. Erker, *Comments Inorg. Chem.* 13 (1992) 111;
- (h) R. Nast, *Coord. Chem. Rev.* 47 (1982) 89.
- [2] (a) S. Back, G. Rheinwald, H. Lang, *J. Organomet. Chem.* 601 (2000) 93;
- (b) W. Frosch, S. Back, K. Köhler, H. Lang, *J. Organomet. Chem.* 601 (2000) 226;
- (c) A. Kovács, G. Frenking, *Organometallics* 18 (1999) 887;
- (d) S. Back, H. Lang, *Organometallics* 19 (2000) 749;
- (e) C.J. Adams, P.R. Raithby, *J. Organomet. Chem.* 578 (1999) 178;
- (f) V.W.-W. Yam, K.-L. Yu, K.M.-C. Wong, K.-K. Cheung, *Organometallics* 20 (2001) 721.
- [3] U. Belluco, R. Bertani, R.A. Michelin, M. Mozzon, *J. Organomet. Chem.* 600 (2000) 37.
- [4] G. Bandoli, A. Dolmella, *Coord. Chem. Rev.* 209 (2000) 161.
- [5] W.-Y. Wong, F.-L. Ting, W.-L. Lam, *Eur. J. Inorg. Chem.* (2001) 623.
- [6] (a) W.-Y. Wong, G.-L. Lu, K.-F. Ng, K.-H. Choi, Z. Lin, *J. Chem. Soc. Dalton Trans.* (2001) 3250;
- (b) W.-Y. Wong, W.-K. Wong, P.R. Raithby, *J. Chem. Soc. Dalton Trans.* (1998) 2761;
- (c) W.-Y. Wong, K.-H. Choi, G.-L. Lu, J.-X. Shi, *Macromol. Rapid Commun.* 22 (2001) 461;
- (d) W.-Y. Wong, S.-M. Chan, K.-H. Choi, K.-W. Cheah, W.-K. Chan, *Macromol. Rapid Commun.* 21 (2000) 453;
- (e) H. Zhang, A.W.-M. Lee, W.-Y. Wong, M.S.-M. Yuen, *J. Chem. Soc. Dalton Trans.* (2000) 3675.
- [7] (a) C.J. Adams, S.L. James, X. Liu, P.R. Raithby, L.J. Yellowlees, *J. Chem. Soc. Dalton Trans.* (2000) 63;
- (b) S.M. AlQaisi, K.J. Galat, M. Chai, D.G. Ray, III, P.L. Rinaldi, C.A. Tessier, W.J. Youngs, *J. Am. Chem. Soc.* 120 (1998) 12149;
- (c) M. Hissler, W.B. Connick, D.K. Geiger, J.E. McGarrah, D. Lipa, R.J. Lachicotte, R. Eisenberg, *Inorg. Chem.* 39 (2000) 447;
- (d) S.L. James, M. Younus, P.R. Raithby, J. Lewis, *J. Organomet. Chem.* 543 (1997) 233;
- (e) C.J. Adams, S.L. James, P.R. Raithby, *Chem. Commun.* (1997) 2155.
- [8] B. Corain, B. Longato, G. Favero, D. Ajò, G. Pilloni, U. Russo, F.R. Kreissl, *Inorg. Chim. Acta* 157 (1989) 259.
- [9] M. Younus, Ph.D. thesis, University of Cambridge, 1996.
- [10] C.V. Ursini, G.H.M. Dias, M. Hörner, A.J. Bortoluzzi, M.K. Morigaki, *Polyhedron* 19 (2000) 2261.
- [11] P.S. Pregosin, R.W. Kunz, in: P. Diehl, E. Fluck, R. Kosfeld (Eds.), *NMR Basic Principles and Progress*, vol. 16, Springer-Verlag, New York, 1979, p. 43.
- [12] J.D. Bradshaw, L. Guo, C.A. Tessier, W.J. Youngs, *Organometallics* 15 (1996) 2582.
- [13] (a) L.R. Falvello, J. Forníes, J. Gómez, E. Lalinde, A. Martín, M.T. Moreno, J. Sacristán, *Chem. Eur. J.* 5 (1999) 474;
- (b) H.-K. Yip, H.-M. Lin, Y. Wang, C.-M. Che, *J. Chem. Soc. Dalton Trans.* (1993) 2939;
- (c) M. Bonamico, G. Dessy, V. Fares, M.V. Russo, L. Scaramuzza, *Cryst. Struct. Commun.* 6 (1977) 39.
- [14] S. Yamazaki, A.J. Deeming, *J. Chem. Soc. Dalton Trans.* (1993) 3051.
- [15] I. Ara, J.R. Berenguer, J. Fornies, E. Lalinde, M.T. Moreno, *J. Organomet. Chem.* 510 (1996) 63.
- [16] W.-Y. Wong, G.-L. Lu, K.-F. Ng, C.-K. Wong, K.-H. Choi, *J. Organomet. Chem.* 637–639 (2002) 159.
- [17] W.L.F. Armarego, D.D. Perrin, *Purification of Laboratory Chemicals*, 4th ed., Butterworth-Heinemann, Guildford, 1996.
- [18] P.J. Kuhba, *Inorg. Chem.* 28 (1990) 78.
- [19] (a) SAINT, Reference manual, Siemens Energy and Automation, Madison, WI, 1994–1996;
- (b) G.M. Sheldrick, SADABS, Empirical Absorption Correction Program, University of Göttingen, 1997.
- [20] G.M. Sheldrick, SHELXTL™, Reference manual, ver. 5.1, Madison, WI, 1997.